

INFRARED SPECTROMETER ACCESSORIES

ATR IR Spectroscopy: An Efficient Technique to Quantitatively Determine the Orientation and Conformation of Proteins in Single Silk Fibers

By Maxime Boulet-Audet, Thierry Lefèvre, Thierry Buffeteau, and Michel Pézolet, Université Laval, Canada and Université de Bordeaux, France

Originally published in *Applied Spectroscopy* **956-962**, Vol. 62 No. 9 (2008), © 2008 Society for Applied Spectroscopy

Polarized attenuated total reflection (ATR) infrared spectroscopy is an efficient technique to determine the orientation and conformation of a large variety of samples, but it is more difficult to apply to very small specimens such as silk fibers. The Golden Gate single-reflection ATR accessory that uses diamond as an ATR element and a focalized beam turns out to be highly efficient to study quantitatively the orientation and conformation of a single silk fibroin filament of the silkworm *Bombyx mori* that is about 10 μm in diameter. For orientation measurements, rotating the sample instead of the electric field greatly simplifies the theoretical analysis and keeps the penetration depth of the infrared radiation constant. A sample holder that can be fitted on the ATR accessory has thus been developed to allow accurate rotation of the sample and to obtain spectra with a low, non-damaging, and reproducible pressure on the fiber. To validate the method, spectra have been recorded as a function of the angle θ between the fiber axis and



Specac's Golden Gate ATR Accessory

the polarization of the incident radiation. The data have been fitted following the cosine square dependency of the absorbance with respect to the angle θ . The procedure has been applied to the spectral components of the amide I bands, as determined from spectral decomposition. Multiple angle measurements turn out to be quite useful to correct systematic angle errors and validate the accuracy of the curve-fitting parameters of the band decomposition. By using the calculated dichroic ratio, a parameter $\langle P_2 \rangle$ of -0.46 ± 0.01 has been calculated for the antiparallel β -sheets and -0.04 ± 0.02 for the

remaining structures. From the orientation-insensitive spectrum A_0 , the amount of β -sheets has been estimated to $49 \pm 3\%$. The results obtained from only two measurements with the electric field of the incident radiation parallel and perpendicular to the fiber axis has demonstrated that ATR spectroscopy can be used routinely in quantitative studies of the molecular orientation and conformation of macromolecules.

Introduction

Fourier transform infrared (FT-IR) spectroscopy is a valuable technique to characterize the molecular conformation and orientation of natural and synthetic macromolecular systems since it can provide high quality spectra of minute amounts of material. In addition, because of the wide variety of available sampling techniques, samples of different size, shape, and physical state can be investigated. Although thin films and solutions can be easily be studied by transmission infrared spectroscopy, it is more difficult to obtain quantitative information about the conformation and orientation of small single fibers such as silkworm and spider silk fibers because their size is often below the diffraction limit of most infrared microscopes. Arrays of tightly packed fibres can be used for transmission experiments, but this method rarely provides high quality spectra because of spectral artifacts due to sample heterogeneities and appreciable leakage of incident radiation through the sample.^{1,2} Finely cut fibers can also be studied by diffuse reflection infrared spectroscopy or by transmission spectroscopy when dispersed in KBr pellets.³ Unfortunately, the microstructure of the fibers is not necessarily preserved with these methods and the information on the molecular orientation is completely lost. Since molecular orientation strongly affects the mechanical properties of natural and synthetic fibers, it is important to develop techniques that allow the

efficient and quantitative determination of molecular orientation *in situ* in single fibers. One of the most efficient techniques to study fiber microstructure by infrared spectroscopy is undoubtedly attenuated total reflection (ATR). The main limitation of most conventional ATR accessories is that several filaments are often necessary to obtain spectra with a sufficiently high signal-to-noise ratio. This strategy has been implemented to examine the conformation of hair fibrous proteins^{4,5} and textile polymers.⁶⁻⁸

Three methods have been used to determine molecular orientation by ATR infrared spectroscopy. The most common one is to keep the sample fixed on the ATR element and to rotate the electric field of the incident radiation. This method is simple to implement since the sample does not have to be moved, but it requires complete knowledge of the components of the electric field in every direction at the surface of the ATR crystal.⁹⁻¹¹ Depending on the thickness of the sample, the ATR element, and the sample, the determination of the electric fields requires the knowledge of the optical properties of the multilayer system.¹² A second method consists of rotating the sample and ATR crystal as a whole,¹³ thus ensuring a constant contact between the sample and the ATR crystal. However, it has been demonstrated that a slight change in the beam path has an important effect on the reproducibility of the measurements.¹⁴ The third method consists of rotating the sample while keeping the beam path and polarization unchanged. The main limitation of this technique is that the contact between the sample and the ATR element can change when the sample is rotated, which strongly affects the intensity of the polarized spectra. To minimize this effect, normalization of the spectra is necessary and can be performed using an orientation-independent band. When such a band is not present, a dye

molecule can be incorporated in the sample to normalize the spectra. Such a procedure has been used to determine qualitatively the orientation of an array of *Bombyx mori* (*B. mori*) silk fibers.^{15,16}

In the present paper, we have taken advantage of the high sensitivity of the Golden Gate single-reflection ATR accessory (Specac Ltd., London, UK) that uses diamond as an ATR element and a focalized beam to study the conformation and orientation of a single silk fibroin filament obtained after degumming cocoon silk produced by the silk worm *B. mori*. This silk fibroin is composed of tyrosine-rich amorphous domains and quasi-crystalline domains formed with the pattern of $(\text{Ala-Gly-Ser-Gly-Ala-Gly})_n$ sequences that are organized into antiparallel pleated β -sheets aligned parallel to the fiber axis.^{17,18} The use of the diamond ATR accessory has allowed the recording of spectra with high signal-to-noise ratios of single *B. mori* silk filaments of about $10\mu\text{m}$ in diameter in a few minutes. To measure

quantitatively the degree of orientation of the proteins, we have developed a new sample holder that allows the precise rotation of the fiber and the application of a low and reproducible pressure on the fiber. With this sample holder, we have successfully determined quantitatively and with a good accuracy the orientation and the secondary structure content of *B. mori* silk fibroin. Although the proposed method was applied to silk fibers, it can be used to study the molecular conformation and orientation of other natural and synthetic fibers as well.

Experimental

Sample Preparation

Cocoons from the silkworm *B. mori* were obtained from the Insects Production Unit of the Canadian Forest Service (Sault Ste. Marie, Ontario, Canada). Raw *B. mori* silk is composed of two fibroin filaments held together by a cementing layer of the protein sericin. To remove the sericin layer, the cocoon silk was degummed

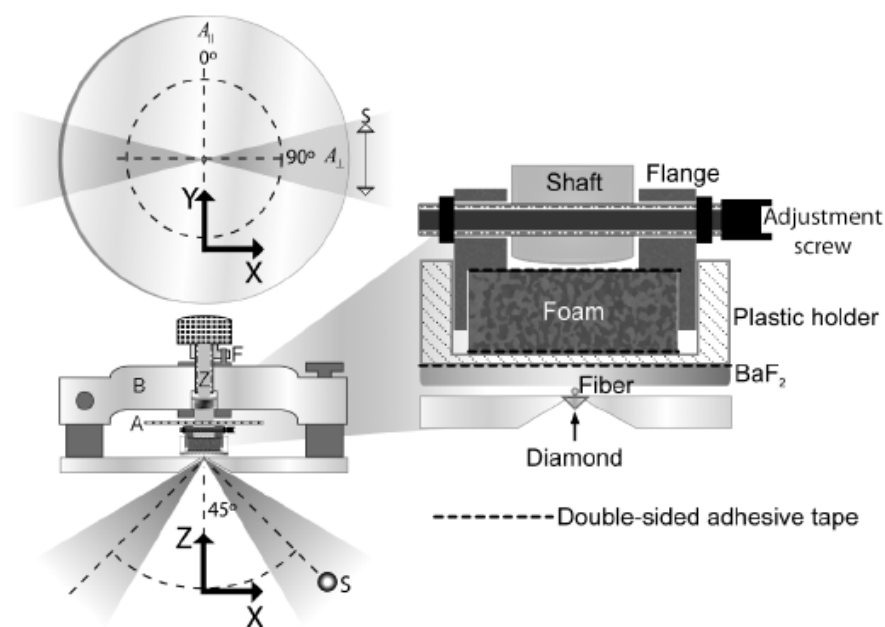


Fig. 1. Coordinate system and mechanical setup used for the sample rotation and dichroism measurements showing the angular wheel (A), the support bridge (B), the shaft (Z) and the elevation stopper (F).

in boiling water containing sodium bicarbonate (0.05% w/v) for 15min. The resulting fibroin filaments were rinsed thoroughly with deionized water and dried under vacuum for a few minutes to remove the excess water. Samples were then stored at 22 ± 1 °C and $65 \pm 5\%$ relative humidity.

Mechanical Setup for Sample Mounting and Rotation

Polarized ATR spectra were recorded for different angles between the electric field of the incident radiation and the fiber axis by rotating the sample. In order to repeatedly have an almost identical contact between the sample and the ATR element for all spectra, the shaft of the Golden Gate ATR accessory was modified to accommodate the sample holder shown in Fig. 1. Another requirement for these experiments was the ability to apply the minimum pressure on the fiber with this setup to obtain spectra with a high enough signal-to-noise ratio without damaging the fiber. The sample holder basically consists of an anvil formed by a barium fluoride (BaF_2) disk attached to a plastic holder of the same diameter with double sided adhesive tape. BaF_2 was chosen for its transparency over the wavenumber domain of interest and for its low refractive index that preserves total internal reflection conditions. Each silk fiber (about 4 cm in length) was positioned as much as possible in the center of the BaF_2 substrate and was gently attached at both ends with adhesive tape on the side of the plastic holder by applying the minimal tension on the fiber to keep it straight and to avoid shrinking of the fiber.

The sample holder was then attached to the shaft of the bridge (B) of the ATR accessory using a circular aluminium flange. To ensure the application of a reproducible low pressure on the sample, a piece of soft low-density polyurethane foam was inserted between the plastic holder and

the aluminium flange. The height of the sample holder was controlled with a screw (Z) embedded in the bridge. A stopper (F) ensures that the shaft is lowered down at exactly the same vertical position each time, which is essential for contact pressure reproducibility. To make sure that the fiber was always perfectly aligned in the center of the ATR crystal, a screw was used for fine lateral adjustments. To prevent baseline deviations due to signal variations over the acquisition time, a background was acquired immediately after each measurement by raising the sample from the ATR crystal. Once the sample was raised, it could be rotated around the shaft and lowered again to acquire a new spectrum at a different angle. A graduated wheel (A) was used to measure the angle between the fiber axis and the electric field of the infrared radiation.

Spectral Acquisition and Treatment

Spectra were recorded using a Nicolet Magna 850 Fourier transform infrared spectrometer (Thermo Scientific, Madison, WI) with a liquid nitrogen cooled narrow-band mercury cadmium telluride (MCT) detector and a Golden Gate ATR accessory. In this apparatus, the infrared beam is focused to a diameter of about 750 μm on the diamond crystal with ZnSe lenses (4X magnification). The electrical field of the infrared beam was polarized perpendicular to the plane of incidence (*s*-polarized or transverse electric) using a ZnSe wire-grid polarizer (Specac Ltd., London, UK). Each spectrum was obtained from 128 scans at a resolution of 4 cm^{-1} using a Happ-Genzel apodization. All spectral operations were performed using GRAMS/AI 8.0 (Thermo Galactic, Salem, NH). The spectra were not smoothed and the only applied baseline correction was an offset at 1730 cm^{-1} . In addition, the spectra were normalized to account for the intensity fluctuations (approximately 10%) due to fiber rotation. This normalization was performed using

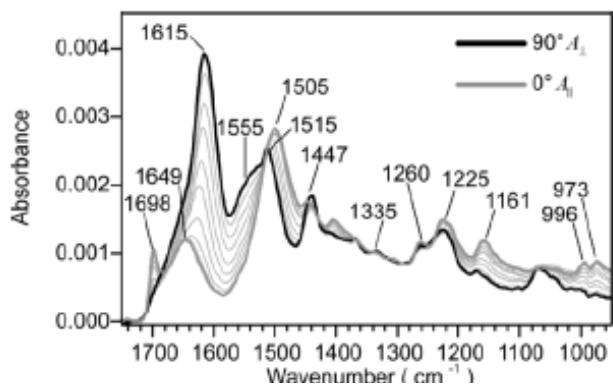


Fig. 2. ATR spectra of a single *B. mori* silk fiber obtained with s-polarized light at different rotation angles of the fiber from 0° (fiber parallel to the electric field) to 90° (fiber perpendicular to the electric field).

the intensity at 1335 cm⁻¹ since the absorbance at this wavenumber was found to be almost insensitive to the orientation.

All spectra were corrected for wavelength dependency of the penetration depth of the infrared radiation. The band fitting iteration routine used in GRAMS is based on a nonlinear algorithm known as the Levenberg-Marquardt method.¹⁹ Pure Gaussian band shapes were chosen for the decomposition. The band positions, determined by a second-derivative, were fixed to ± 0.5 cm⁻¹ and the bandwidths were allowed to vary to ± 5 cm⁻¹. The initial bandwidths of the different components were estimated by manual fitting of the most appropriate spectrum recorded at 0° or 90°, whereas the initial intensities were set to 0. To ensure reliable band decomposition of a set of spectra recorded for different orientations of the fiber, all curve-fittings were done using the same set of initial parameters and limits.

Results and Discussion

Figure 2 shows the ATR spectra between 950 and 1750 cm⁻¹ of a single fibroin filament of degummed *B. mori* cocoon silk obtained with the

Position (cm ⁻¹)	Assignment ^a	Preferential Orientation	References
1698	Amide I, β -sheets		15,22,45,46
1649	Amide I, unordered		24-26,47
1615	Amide I, β -sheets	⊥	15,22,28,32
1594	N(C-C) ring, tyrosine		30,48
1555	Amide II, β -sheets	⊥	22,24
1527	Amide II, unordered		24,26,27,29
1515	ν (C-C) and δ (CH), tyrosine		30,31
1505	Amide II, β -sheets		24-29
1469	$\delta_{as}(\text{CH}_3)$, alanine, β -sheets		22,30
1447	$\delta(\text{CH}_2)$, (AG) _n		22
1437	$\delta(\text{CH}_2)$, (AG) _n β -sheets	⊥	22
1406	w(C ₆ H ₂), (AG) _n		22,49
1369	$\delta_s(\text{CH}_3)$, (AG) _n		22
1335	$\delta_s(\text{CH}_3)$, (AG) _n		22
1260	Amide III, β -sheets		22,29,32-34
1225	Amide III, unordered		29,32,33
1161	ν (N-C _α) and δ (H _α), (AG) _n		22
1103	Tyrosine		32
1070	ν (C-C)		32
1055	ν (C-C)		32
1014	r(CH ₂), tyrosine		32
996	r(CH ₂), (AG) _n β -sheets		22,32
973	r(CH ₂), (AG) _n β -sheets		22,32

^a Abbreviations used: ν , stretching; δ , bending; w, wagging; r, rocking; as, asymmetric; s, symmetric.

Table I. Assignment and orientation dependence of the observed bands in the polarized ATR spectra of *B. mori* silk.

s-polarized light parallel and aligned at different angles from 0° (parallel spectrum, A_{||}, and along the y-axis) to 90° (perpendicular spectrum, A_⊥, along the x-axis). As can be seen, the use of the Golden Gate accessory allows the recording of spectra of a 10 μm fiber with a very high signal-to-noise ratio in a few minutes. The spectra at 0° and 90° are in good agreement with those of Garside et al. obtained on an array of *B. mori* silk fibers.¹⁵ The most intense bands are due to the

amide I, II, and III vibrations and are observed in the 1600-1700, 1500-1560, and 1200-1300 cm^{-1} spectral regions, respectively. The assignment of the major bands of *B. mori* silk is given in Table I. Figure 2 clearly shows that the sample is anisotropic and that the silk fibroin is highly oriented, as reported previously by various techniques.^{17,18,20} In the amide I region, it is acknowledged that the coupling between the four peptide bonds in the unit cell of the antiparallel pleated β -sheet results in four normal modes labelled $\nu(0,0)$, $\nu_{\parallel}(0,\pi)$, $\nu_{\perp}(\pi,0)$ and $\nu_{\perp}(\pi,\pi)$.^{21,22} The first character in the parentheses indicates whether the vibrations of two adjacent amide groups in the same chain are in-phase (0) or out-of-phase (π), while the second character indicates the phase between two amide groups located in adjacent chains.²¹ The $\nu(0,0)$ mode is infrared inactive, whereas the $\nu_{\perp}(\pi,\pi)$ is too weak to be observed. The $\nu_{\perp}(\pi,0)$ is found at 1615 cm^{-1} in Fig. 2, and the transition moment associated with this vibration is perpendicular to the peptide chain. The $\nu_{\parallel}(0,\pi)$ mode is observed at 1698 cm^{-1} and is parallel to the chain axis. The frequency of the perpendicular component is quite sensitive to the strength of the hydrogen bonding and can appear between 1615 to 1637 cm^{-1} .²³ However, the low wavenumber position found in this study is essentially due to an optical effect occurring in ATR spectroscopy with a diamond crystal when

the refractive index of the sample is too high (unpublished results). The broad component at 1649 cm^{-1} is assigned to the protein chains present in the amorphous phase of silk and is due to other secondary structures such as 3_1 -helices, β -turns, or unordered structures that are not resolved in the spectra.

As for the amide I vibration, the amide II band clearly shows components with parallel and perpendicular dichroism due to coupled modes in the β -sheets. The perpendicular component arises at 1555 cm^{-1} while the parallel component is located at 1505 cm^{-1} , in agreement with the results obtained using regenerated films.^{22,24-29} An amide II component due to the amorphous phase is also observed at 1527 cm^{-1} by Fourier self-deconvolution (data not shown), as observed for regenerated fibroin films.^{24,26,27,29} Its intensity is basically independent of orientation of the fiber (data not shown). The small shoulder at 1515 cm^{-1} is typical of the C-C stretching vibration of tyrosine residues.^{30,31} The amide III band can be decomposed into two components, one due to the β -sheet conformation at 1260 cm^{-1} and one to the other secondary structures at 1225 cm^{-1} .^{22,29,32-34} The 1161 cm^{-1} band can be assigned to the N-C α stretching vibration, which is consistent with its parallel dichroism.²² The 972 and 993 cm^{-1} bands due to the CH_2 rocking modes are typical of (Ala-

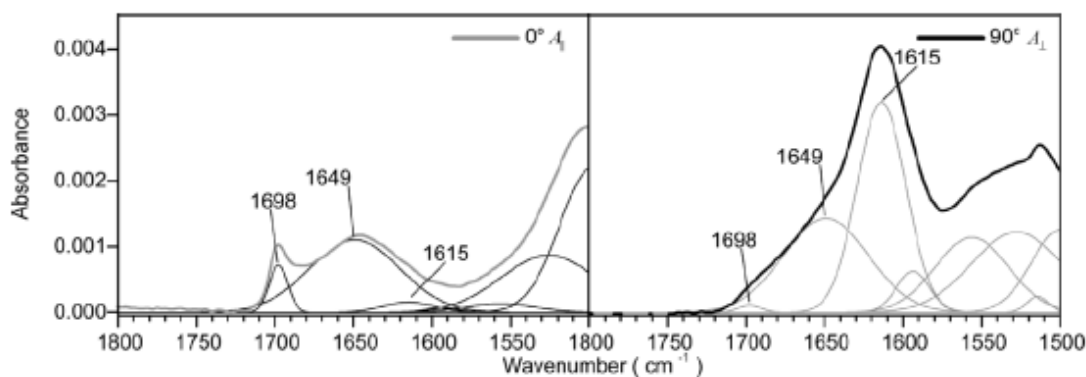


Fig. 3. Spectral decomposition of the experimental spectra of a single *B. mori* silk fiber recorded at 0° and 90°

Gly)_n sequences in a β -sheet conformation and exhibit a parallel dichroism.²² The relative intensity between the 973-996 cm⁻¹ bands and the 1014 cm⁻¹ one due to tyrosine has been used as a marker for the (AG)_n sequence conformation.³²

To obtain more quantitative information about the degree of orientation of the secondary structures, the amide I region of the polarized spectra obtained at various rotation angles (Fig. 2) was decomposed into three components as shown in Fig. 3. To ensure an accurate band fitting, it was necessary to add components at lower wavenumbers due to tyrosine side-chain and amide II vibrations.

Figure 3 shows typical decomposed spectra for a fiber aligned at 0° and 90°. These spectra clearly confirm that the β -sheets are highly oriented in *B. mori* silk since the 1615 and 1698 cm⁻¹ components almost completely disappear in the 0° and 90° spectra, respectively. On the other hand, the amorphous phase appears to be almost randomly oriented since the 1649 cm⁻¹ component does not display any significant dichroism. Since for a given vibration, the absorbance is proportional to the square of the scalar product between the transition moment (*M*) and the electric field of the infrared radiation (*E*), the absorbance should follow a cosine square function of the angle, θ , between the fiber axis and the electric field such that²¹

$$(1) \quad A(\theta) = A_{\parallel} \cos^2(\theta - \delta) + A_{\perp} \sin^2(\theta - \delta)$$

where *A*_∥ and *A*_⊥ are absorbances measured when the infrared radiation is polarized parallel (0°) and perpendicular (90°) to the fiber axis, respectively, and δ is a phase factor that accounts for the error in the angular positioning of the fiber. The experimental absorbances of the

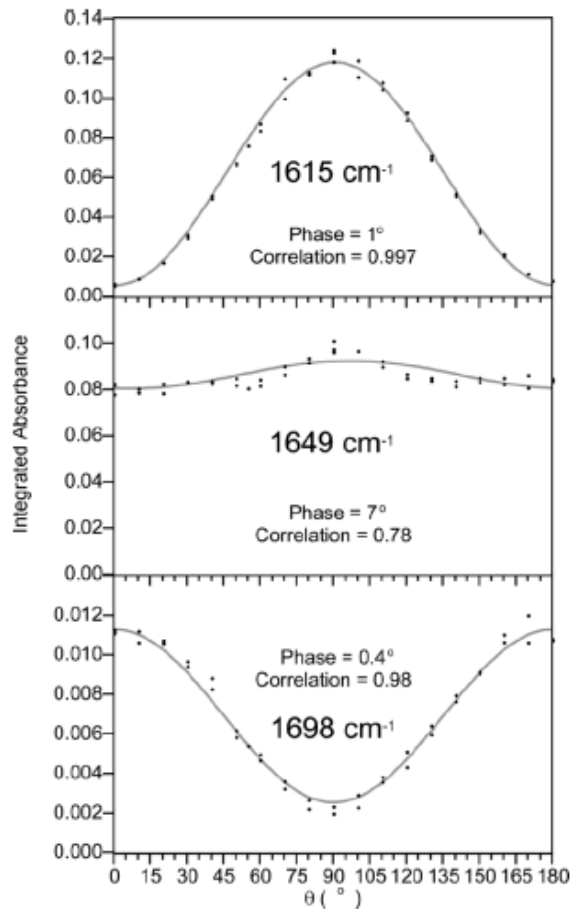


Fig. 4. Integrated absorbance of the 1615, 1649, and 1698 cm⁻¹ band components as a function of the angle θ between the fiber axis and the electric field of the infrared radiation. The correlation with Eq. 1 is also shown.

components at 1615, 1649, and 1698 cm⁻¹ are plotted as a function of θ in Fig. 4. As can be seen, the data follow Eq. 1 with very good correlation coefficients, even for the weakest β -sheet component at 1698 cm⁻¹. In addition, the small value of the phase factor, which is not absolutely necessary to obtain reliable correlations, reveals that the fiber can be positioned quite accurately. These excellent results clearly demonstrate that, even though the absorbance of the amide band is lower than 0.004 for a single *B. mori* silk fiber, the use of a diamond ATR accessory is very effective

to study protein orientation in silk and that the designed sample holder ensures a reproducible and non-damaged contact between the fiber and the ATR crystal. It is important to mention here that curve-fittings of the polarized spectra using the same set of spectra but with unlocked band parameters (shapes, widths, and positions) lead to better adjustments of the experimental spectra but did not yield as good results in terms of intensity variation of the components as a function of θ . The most relevant criterion to assess the validity of the band decomposition is not the quality of the curve-fitting of the experimental spectra, but rather the fact that the intensity of each component of the amide I band follows Eq. 1 as much as possible. As a matter of fact, band fitting could easily lead to wrong results (bad correlations with Eq. 1) if band parameters are not rigorously constrained. Table II shows the values of A_{\parallel} and A_{\perp} determined from fitting Eq. 1. The errors given in this table come from the quality of the fit of Eq. 1 and thus take into account the error on the fiber positioning, and the validity of the normalization of the spectra, and the band fitting of the spectra. Although the resulting A_{\parallel} and A_{\perp} are more accurate because they were obtained from 36 measurements (at 18 angles), the recording of only two spectra with the incident electric field oriented parallel and perpendicular to the fiber axis also leads to satisfactory determination of A_{\parallel} and A_{\perp} (see below).

For a system such as silk showing uniaxial symmetry of orientation around the fiber axis, it

is possible to quantify the degree of orientation of the transmission moment of a given vibration from the above values of A_{\parallel} and A_{\perp} . The dichroic ratio R is obtained using Eq. 2 allows the calculation of the second moment $\langle P_2(\cos \gamma) \rangle$ or $\langle P_2 \rangle$ of the orientation distribution function expressed as a sum of Legendre polynomials in $\cos \gamma$, where γ is the angle between M and E (Eq. 3):³⁵

$$(2) \quad R = \frac{A_{\parallel}}{A_{\perp}}$$

$$(3) \quad \langle P_2(\cos \gamma) \rangle = \frac{3\langle \cos^2 \gamma - 1 \rangle}{2} = \frac{R - 1}{R + 2}$$

The parameter $\langle P_2 \rangle$ is often called the order parameter. For an isotropic sample, $\langle P_2 \rangle = 0$. For an orientated sample, $\langle P_2 \rangle = 1$ if all the transition moments are perfectly orientated parallel to the fiber axis, while $\langle P_2 \rangle$ is -0.5 and 0 for perfect orientation at 90° and 54.7° , respectively. The values of R and $\langle P_2 \rangle$ calculated for the 1615, 1649, and 1698 cm^{-1} bands are given in Table II. The transmission moment of the 1615 cm^{-1} component of the antiparallel β -sheets shows a high degree of orientation perpendicular to the fiber axis with a $\langle P_2 \rangle$ value of -0.46 ± 0.01 , which is close to the value of -0.45 ± 0.02 obtained by the Raman spectromicroscopy.³⁶ For the parallel component of the β -sheets at 1698 cm^{-1} , a $\langle P_2 \rangle$ value of 0.56 ± 0.04 is calculated. Assuming that the parallel and perpendicular components of the β -sheets are perfectly orthogonal, the $\langle P_2 \rangle$ value

Position (cm^{-1})	Width (cm^{-1})	A_{\parallel}	A_{\perp}	R	$\langle P_2 \rangle$	Integrated absorbance (A_0)	Relative Area
1698	15	0.0114 ± 0.0002	0.0024 ± 0.0002	4.7 ± 0.05	0.56 ± 0.04	0.0056 ± 0.0006	$3 \pm 1\%$
1649	64	0.080 ± 0.001	0.092 ± 0.001	0.87 ± 0.03	-0.04 ± 0.02	0.088 ± 0.003	$51 \pm 2\%$
1615	35	0.0052 ± 0.0007	0.1178 ± 0.0004	0.04 ± 0.01	-0.46 ± 0.01	0.082 ± 0.001	$46 \pm 2\%$

Table II. Polarized absorbances (A_{\parallel} and A_{\perp}), dichroic ration (R), order parameter ($\langle P_2 \rangle$), and relative area of the major components of the amide I band obtained from the fit of Eq. 1.

of the 1698 cm^{-1} component can in theory be calculated from that of the 1615 cm^{-1} component. According to the Legendre addition theorem and providing that the symmetry is perfectly uniaxial around the fiber axis, the value of $\langle P_2 \rangle$ for the 1698 cm^{-1} component should be 0.92 instead of 0.56.³⁷ This discrepancy might be due to the fact that the β -sheets in silk may be distorted or twisted, as is often found in proteins.³⁸ In addition, the error on the dichroic ratio is higher for this component since it is quite weak, especially in the perpendicular spectrum. The transmission moments associated with the amide I component at 1649 cm^{-1} appear to be almost randomly orientated since $\langle P_2 \rangle$ value for this band is near 0 at -0.04 ± 0.02 , which suggests that the amorphous phase is almost unorientated.

The above results obtained at several rotation angles of the fiber are very useful to validate both the efficiency of the sample holder and the band-fitting procedure of the polarized spectra. However, it is well known that only the A_{\parallel} and A_{\perp} spectra are necessary to calculate the order parameter $\langle P_2 \rangle$ (see Eqs. 2 and 3). Consequently, in routine analysis, only two spectra have to be recorded. The reproducibility of the method was thus estimated on different cocoon fibers for two polarized spectra only. Figure 5 shows the A_{\parallel} and A_{\perp} spectra of five different cocoon monofilaments. For comparison purposes, the

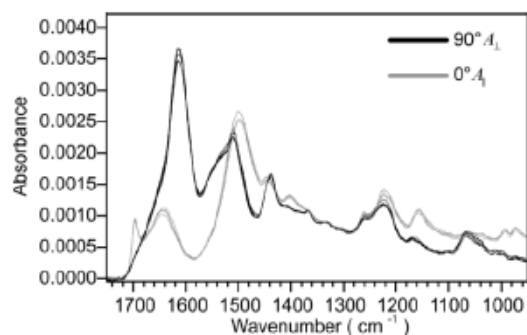


Fig. 5. Normalized spectra of five different *B. mori* silk fibers recorded at 0° and 90° .

spectra have been normalized at 1335 cm^{-1} , which allows differences in the sample specimens and experimental errors to be taken into account. As judged from the variation of the absorbance, the reproducibility of the measurement is very good, the dichroic ratio R and order parameter $\langle P_2 \rangle$ calculated for the 1615 cm^{-1} band being 0.06 ± 0.01 and -0.46 ± 0.01 , respectively.

To obtain more insights into the conformation of the silk fibroins, an orientation-independent or structural absorbance spectrum (A_0) can be calculated from the parallel and perpendicular polarized spectra using Eq. 4.³⁹ Since the $\langle P_2 \rangle$ value is 0 at 54.7° , the spectrum recorded at this angle should be equivalent to A_0 :

$$(4) \quad A_0 = \frac{A_{\parallel} + 2A_{\perp}}{3} = A(54.7^\circ)$$

The structural spectrum recorded at 54.7° and the one calculated from A_{\parallel} (0°) and A_{\perp} (90°) of Fig. 2 are shown in Fig. 6. As can be seen, the agreement between the two spectra is very good, confirming again the accuracy of the values of A_{\parallel} and A_{\perp} obtained from the fit of Eq. 1 and the presence of a cylindrical isotropy around the fiber axis. The small deviation between the two spectra is due to the small uncertainty on A_{\parallel} and A_{\perp} in addition to the error on fiber position.

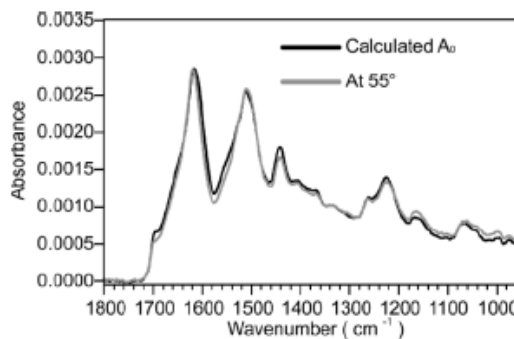


Fig. 6. ATR spectrum of a single fiber recorded at 55° and the orientation-independent spectrum A_0 calculated from the 0° and 90° spectra.

The spectrum A_0 can be used to estimate the relative amount of each component of the amide I band. Assuming that all components have the same molar absorptivity,⁴⁰⁻⁴² the proportion of each secondary structure can be estimated from the relative integrated intensity of the different components in the A_0 spectrum. The results obtained for the three components of the amide I band are given in Table II. By adding the integrated absorbance of the 1615 and 1698 cm^{-1} components, the content of β -sheets is found to be $49 \pm 3\%$. If the isotropic spectrum is calculated from the spectra of Fig. 5, the average value for β -sheet content is $48 \pm 3\%$. The content of β -sheets found by infrared spectroscopy then appears close to the values of $50 \pm 3\%$ and $56 \pm 5\%$ determined from Raman measurements by Lefèvre et al.³⁶ and Gillespie et al.,⁴³ respectively. On the other hand, Asakura and co-workers have shown from solid-state nuclear magnetic resonance (NMR) measurements that the amount of β -sheets is 38%.⁴⁴ Overall, the level of orientation and the content of the β -sheets presented in this work are in fairly good agreement with the literature.

Conclusion

This work presents a convenient approach for routine analysis of small single fibers that can overcome the experimental limitations of conventional ATR and transmission experiments. The only requirement is to assure that the contact between the sample and the ATR crystal is

References

1. R. Prost, *Clay Clay Miner.* **21**, 363 (1973).
2. A. Garton, D. J. Carlsson, and D. M. Wiles, *Text. Res. J.* **51**, 28 (1981).
3. V. Nimmen, *Vib. Spectrosc.* **46**, 63 (2008).
4. D. J. Lyman and J. Murray-Wijelath, *Appl. Spectrosc.* **59**, 26 (2005).

perfectly reproducible, which can be achieved by using the sample holder developed in our laboratory. Although two spectra are sufficient to calculate the orientation order parameter and the isotropic spectrum, the robustness of the reproducibility can be ascertained from measurements at different angles as described in this study. Multiple angle measurements is also advantageous for validating the band-fitting procedure, which is a necessary step to extract quantitative information relative to the different vibrational amide I modes. This approach, which makes use of diamond as the ATR element accessory, can even be used on smaller fibers such as spider silk. Therefore, it is anticipated that the textile industry, for example, could take advantage of this technique. Further studies on the comparison of the conformation and orientation of different types of silk as well as the effect of humidity and mechanical drawing are in progress in our laboratory.

Acknowledgments

This work was supported by grants from the National Sciences and Engineering Research Council (NSERC) of Canada and the Fonds Québécois de Recherche sur la Nature et les Technologies (FQRNT). The authors express their gratitude to François Lapointe, Jean-François Rioux-Dubé, and Sébastien Blanchet for their valuable technical support and to Christian Pellerin for helpful discussions.

5. E. G. Bartick, M. W. Tungol, and J. A. Reffner, *Anal. Chim. Acta.* **228**, 35 (1994).
6. V. Causin, C. Marega, G. Guzzini, and A. Marigo, *Appl. Spectrosc.* **58**, 1272 (2004).
7. A. V. Savitsky, I. A. Gorshkova, and K. Kober, *J. Macromol. Sci. Phys. B* **37**, 119 (1998).
8. J. S. Church and D. J. Evans, *J. Appl. Polym. Sci.* **57**, 1585 (1995).

9. V. Premnath, *Macromolecules* **28**, 5139 (1995).
10. P. Schmidt, M. Raab, J. Kolarik, and K. J. Eichhorn, *Polym. Test.* **19**, 205 (2000).
11. D. Marsh, *Biophys. J.* **72**, 2710 (1997).
12. F. Picard, T. Buffeteau, B. Desbat, M. Auger, and M. Pézolet, *Biophys. J.* **76**, 539 (1999).
13. J. P. Hobbs, C. S. P. Sung, K. Krishnan, and S. Hill, *Macromolecules* **16**, 193 (1983).
14. F. M. Mirabella, *Appl. Spectrosc.* **42**, 1258 (1988).
15. P. Garside, S. Lahlil, and P. Wyeth, *Appl. Spectrosc.* **59**, 1242 (2005).
16. P. Garside, and P. Wyeth, *Appl. Phys. A: Mater.* **89**, 871 (2007).
17. R. E. Marsh, R. B. Corey, and L. Pauling, *Biochem. Biophys. Acta* **16**, 1 (1955).
18. B. Lotz and H. D. Keith, *J. Mol. Biol.* **61**, 201 (1971).
19. D. W. Marquardt, *J. Soc. Ind. Appl. Math.* **11**, 431 (1963).
20. E. Suzuki, *Spectrochim. Acta, Part A* **23**, 2303 (1967).
21. T. Miyazawa, *J. Chem. Phys.* **32**, 1647 (1960).
22. W. H. Moore and S. Krimm, *Biopolymers* **15**, 2465 (1976).
23. Y. N. Chirgadze and N. A. Nevskaya, *Biopolymers* **15**, 2465 (1976).
24. M. Sonoyama and T. Nakano, *Appl. Spectrosc.* **54**, 968 (2000).
25. S. Y. Venyaminov and N. N. Kalnin, *Biopolymers* **30**, 1259 (1990).
26. L. Jeong, K. Y. Lee, J. W. Liu, and W. H. Park, *Int. J. Macromol.* **38**, 140 (2006).
27. Q. Lv, C. B. Cao, Y. Zhang, X. L. Ma, and H. S. Zhu, *J. Appl. Polym. Sci.* **96**, 2168 (2005).
28. W. S. Muller, L. A. Samuelson, S. A. Fossey, and D. L. Kaplan, *Langmuir* **9**, 1857 (1993).
29. H. Yoshimizu and T. Asakura, *J. Appl. Polym. Sci.* **40**, 1745 (1990).
30. A. Barth, *Prog. Biophys. Mol. Bol.* **74**, 141 (2000).
31. Y. N. Chirgadze, O. V. Fedorov, and N. P. Trushina, *Biopolymers* **14**, 679 (1975).
32. P. Taddei and P. Monti, *Biopolymers* **78**, 249 (2005).
33. J. Z. Shao, J. H. Zheng, J. Q. Liu, and C. M. Carr, *J. Appl. Polym. Sci.* **96**, 1999 (2005).
34. T. Asakura, A. Kuzuhara, R. Tabeta, and H. Saito, *Macromolecules* **18**, 1841 (1985).
35. T. Buffeteau and M. Pézolet, "Linear Dichroism in Infrared Spectroscopy", in *Handbook of Vibrational Spectroscopy*, J. M. Chalmers and P. R. Griffiths, Eds. (John Wiley and Sons, London, 2002), pp. 693-710.
36. T. Lefèvre, M. E. Rousseau, and M. Pézolet, *Biophys. J.* **92**, 2885 (2007).
37. T. Buffeteau and M. Pézolet, "Infrared Linear Dichroism of Polymers", in *Vibrational Spectroscopy of Polymers: Principles and Practice*, N. J. Everall, J. M. Chalmers, and P. R. Griffiths, Eds. (John Wiley and Sons, London, 2007), pp. 255-281.
38. C. Chothia, *J. Mol. Biol.* **75**, 295 (1973).
39. P. G. Schmidt, *J. Polym. Sci. Part A* **1**, 1271 (1963).
40. T. Buffeteau, E. Le Calvez, S. Castano, B. Desbat, D. Blaudez, and J. Dufourcq, *J. Phys. Chem. B.* **104**, 4537 (2000).
41. F. Dousseau and M. Pézolet, *Biochemistry* **29**, 8771 (1990).
42. Y. N. Chirgadze and E. V. Brazhnikov, *Biopolymers* **13**, 1701 (1974).
43. D. B. Gillespie, C. Viney, and P. Yager, *Am. Chem. Soc. Symp. Ser.* **544**, 155 (1994).
44. T. Asakura, J. M. Yao, T. Yamane, K. Umemura, and A. S. Ulrich, *J. Am. Chem. Soc.* **124**, 8794 (2002).

45. H. Teramoto and M. Miyazawa, *Biomacromolecules* **6**, 2049 (2005).
46. T. Miyazawa and E. R. Blout, *J. Am. Chem. Soc.* **83**, 712 (1961).
47. E. Goormaghtigh, V. Cabiaux, and J. M. Ruyschaert, "Determination of soluble and membranes Protein Structure by Fourier Transform Infrared Spectroscopy II. Experimental Aspects, Side Chain Structure, and H/D Exchange", in *Physicochemical Methods in the study of Biomembranes*, H. J. Hilderson and G. R. Ralston, Eds. (Plenum Press, New York, 1994), pp. 363-403.
48. X. Hu, D. Kaplan, and P. Cebe, *Macromolecules* **39**, 6161 (2006).
49. A. Brack and G. Spach, *Biopolymers* **11**, 563 (1972).

Specac Ltd

River House
97 Cray Avenue, Orpington
Kent, BR5 4HE.
United Kingdom
T: +44 (0) 1689 873134
F: +44 (0) 1689 878527
E: sales@specac.co.uk

Specac Inc

T: 1 800 477 2558
E: sales@specac.com